Scheme III

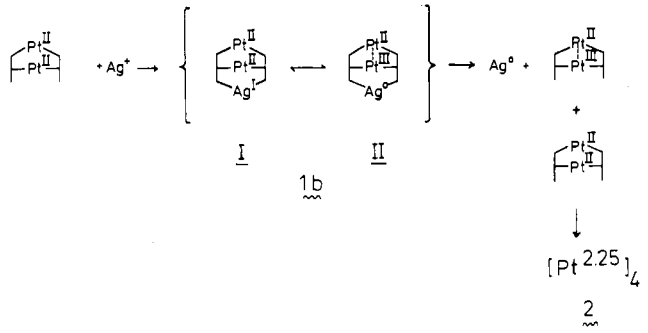

on this basis also more likely. Although we cannot fully exclude possible alternative descriptions of the disorder in this structure, we are reasonably positive that **1b** should be formulated as *cis*-$\{[(NH_3)_2Pt(1\text{-}MeU)]_2Ag_2(NO_3)_{2.5}(OH_2)_{0.5}\}(NO_3)_{1.5}$.

Pt_2,Ag,L_2 as a Precursor Complex. We have previously discussed changes in intramolecular Pt–Pt separations in dinuclear uracilato- or thyminato-bridged complexes in terms of effects of tilt angles between the Pt planes, of torsional angles about the Pt–Pt vectors, and of "manipulations" (metal coordination, H bonding) of the available O2 oxygens.[25] Considering the results of the structure determination of **1b** *and* its solution behavior, it is tempting to also use electronic arguments and to postulate that **1b** (and its equivalent in solution, **1b'**, respectively) is a direct precursor of $Pt^{2.25}$–1-MeU blue. The substantial shortening of Pt–Pt in **1b** on Ag binding (almost halfway between the distance in the $[Pt^{2.0}]_2$ starting compound and that in $Pt^{2.25}$–1-MeU blue) suggests that one electron of the HOMO of the Pt_2 core is already "on its way" to Ag^+; hence, a situation is approached that might be described by the resonance structures I and II given in Scheme III. On the basis of redox potentials ($E°_{Pt(2.0)/Pt(2.25)}$ = 780 mV,[26] $E°_{Ag(0)/Ag(I)}$ = 810 mV) electron transfer to Ag(I) certainly is not unexpected. Attempts to monitor the decay of **1b** rather than the formation of **2** spectroscopically in solution, e.g. via a CT band of **1b**, were unsuccessful, because no such band could be identified between 300 and 900 nm.[27] A low complex stability of **1b** and/or the need of higher concentrations (to accomplish dimer-to-dimer association) might account for this failure. Studies are under way to find out whether the results reported here can be substantiated for the interaction of dinuclear Pt complexes with other redox-active transition metals.

Acknowledgment. This work has been supported by the Deutsche Forschungsgemeinschaft and the Fonds der Chemischen Industrie. We thank I. Dettinger for experimental assistance.

Registry No. **1b**, 107846-63-9; **2**, 92220-63-8; *cis*-$[(NH_3)_2Pt(1\text{-}MeU)]_2(NO_3)_2$, 85886-74-4; $AgNO_3$, 7761-88-8; $Ce(SO_4)_2$, 13590-82-4; $Fe(NO_3)_3$, 10421-48-4; Cu^{2+}, 15158-11-9.

Supplementary Material Available: Listings of positional parameters, distances and angles of 1-MeU ligands and nitrates, possible H-bonding interactions, and conformational parameters and a proposed reaction scheme between $[Pt^{2.0}]_2$ and Cu^{II}–O_2 (5 pages); a listing of observed and calculated structure factors (14 pages). Ordering information is given on any current masthead page.

(25) Schöllhorn, H.; Thewalt, U.; Lippert, B. *Inorg. Chim. Acta* **1984**, *93*, 19.

(26) Micklitz, W.; Riede, J.; Müller, G.; Lippert, B., to be submitted for publication in *Inorg. Chem.*

(27) On the basis of the color of **1b** in the solid state (golden yellow, tint toward orange as opposed to pale yellow for $[Pt^{2.0}]_2$) one might expect an absorption in the 420–490-nm range.

Contribution from the Chemical Physics Group,
Tata Institute of Fundamental Research, Colaba, Bombay 400 005, India

Electronic Structure of Hemin Chloride in Pyridine and Pyridine–Chloroform Solution: Proton NMR Study

L. B. Dugad, O. K. Medhi,† and Samaresh Mitra*

Received February 12, 1986

Variable-temperature ^1H NMR measurements at 500 MHz on (protoporphyrinato)iron(III) chloride (hemin chloride) in pure dry pyridine and a pyridine–chloroform mixture are reported. In freshly prepared solution the autoreduction of the ferric ion in hemin chloride is minimal, and only two iron(III) complexes are generally observed. The high-spin methyl proton resonances in the 50–60 ppm range are believed to be associated with six-coordinated (pyridine)hemin chloride while the low-spin methyl resonances in the 15–25 ppm range refer to the bis(pyridine)ferric protoporphyrin complex. The temperature dependence of the proton resonances conform reasonably well to the spin assignments. Addition of chloroform to this hemin–pyridine solution slowly decreases the concentration of the high-spin complex, which finally disappears at a large excess of chloroform. The "low-spin" complex with methyl resonances in the 15–25 ppm range in the pyridine–chloroform solution shows anomalous temperature dependence, which has been satisfactorily interpreted quantitatively on a thermal spin equilibrium between $S = {}^5/_2$ and $S = {}^1/_2$.

Introduction

The protein control of the axial ligation mode of the heme group in hemoproteins has resulted in a multiplicity of functions for the hemoproteins, such as oxygen transport in hemoglobin, electron transport in cytochrome *c*, and oxygen redox chemistry in peroxidases.[1,2] The ability to perform such diverse functions has been attributed to the easy accessibility of different oxidation and spin states of the iron in the complexed state.[3,4] The nature of the axial ligands and their reactivity toward binding iron in heme play an important role in stabilizing various oxidation and spin states.

Investigations of structure and structure-related electronic properties of the heme prosthetic group in hemoproteins and model systems have provided considerable insight into the biochemical functions of these macromolecules. The study of ligand-exchange reactions and concomitant structural changes has in particular attracted considerable attention. Such studies can be effectively

† Permanent address: Chemistry Department, Gauhati University, Guwahati 781 014, India.

(1) Smith, K. M. *Acc. Chem. Res.* **1979**, *12*, 374.
(2) Taylor, T. G. *Acc. Chem. Res.* **1981**, *14*, 102.
(3) Reed, C. A. *Met. Ions Biol. Syst.* **1978**, *7*, 277.
(4) Scheidt, W. R.; Reed, C. A. *Chem. Rev.* **1981**, *81*, 543.

0020-1669/87/1326-1741$01.50/0

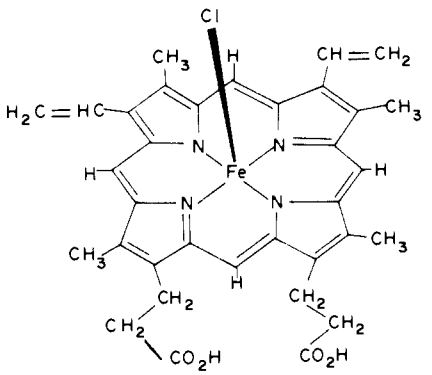

Figure 1. Structure of hemin chloride.

carried out by NMR spectroscopy, which is very sensitive to the changes in the structural and electronic properties of the heme chromophore in solution.[5]

(Protoporphyrinato)ferric chloride (henceforth called hemin chloride, Figure 1) in pyridine and pyridine–chloroform solutions provides a simple and convenient system to investigate some of these structural and electronic features by ^{1}H NMR spectroscopy in solution. Epstein et al.[6] and Moss et al.[7] had reported in frozen solution at 77 K the Mössbauer spectrum of hemin chloride in neat pyridine and observed that the iron existed in two different oxidation states, namely in high-spin ferric and low-spin ferrous forms. The nature and possible structure of these species were not discussed. Later Weightman et al.[8] reported UV–visible and ^{1}H NMR studies at room temperature on hemin chloride in pure pyridine. The ^{1}H NMR measurements were done at 60 MHz but the spectrum showed clear evidence of high-spin iron(III) species, believed to be (pyridine)hemin chloride. In addition, resonances indicative of low-spin iron(III) and a small amount of low-spin iron(II) formed over a period of time were also inferred. The optical spectral studies also supported existence of these species. Weightman et al. further observed that a fast exchange existed between the low-spin iron(II) and iron(III) porphyrin complexes while the exchange between the high- and low-spin ferric complexes was slow. Lack of temperature-dependent and high-resolution studies however prevented detailed characterization of these species formed in solution.

Hill and Morallee[9] had studied ^{1}H NMR of hemin chloride in pyridine–chloroform solution and claimed to observe high-spin iron(III) species. They observed however resonances ascribed to "low-spin" iron(III) species, which showed anomalous temperature dependence. They tentatively assigned this anomaly to a reversible thermal spin equilibrium between $S = {}^3/_2$ and $S = {}^1/_2$ of the ferric ion. This is rather a novel suggestion since generally iron(III) heme proteins involve an $S = {}^5/_2$, $S = {}^1/_2$ thermal spin equilibrium.[10-12]

In this paper a detailed variable-temperature ^{1}H NMR study (at 500 MHz) of hemin chloride in pure pyridine and pyridine–chloroform solutions is reported to understand the nature and characteristic features of the species formed in solution. Finally the temperature dependence of the isotropic proton shift (IPS) is theoretically analyzed on a crystal field model[13-16] to understand the electronic properties of the metal ion and the spin equilibrium involved in these systems.

Experimental Section

Hemin chloride was purchased from Aldrich Chemical Co. and was used without further purification. The purity of the sample was however checked by NMR and visible spectra. The proton NMR spectra were recorded on a Bruker AM 500-MHz FT NMR spectrometer. The temperatures were measured accurately within ±0.5 °C. The isotropic shifts are in ppm and are with respect to Me_4Si as internal standard. Positive values of the shifts indicate downfield shifts. The typical concentrations of hemin chloride in pyridine solutions, used in the present work, ranged between 20 and 30 mM. All the measurements were made on freshly prepared solution.

Results and Discussion

Hemin Chloride in Pyridine. A typical trace of the proton magnetic resonance (^{1}H NMR) spectrum of hemin chloride in pyridine-d_5 solution is shown in Figure 2. The spectrum is similar to that reported by Weightman et al.[8] except that better resolution and additional details have been achieved in the present study. The assignment of various resonances for the high- and low-spin ferric heme species are based on those documented in literature.[8,9,17] The spectrum shows clearly two sets of ring methyl proton resonances, one lying in the 50–60 ppm range and another in the 10–20 ppm range. We consider here mainly the ring methyl proton resonances as these are distinct, easily identifiable, and hence convenient for the purpose of detailed analysis. The downfield ring methyl resonances lying in the 50–60 ppm range are typical of high-spin ferric porphyrins.[14,17,18] Their temperature dependence (Figure 3a) is also similar to that observed for high-spin (protoporphyrinato)ferric complexes (see below). The other set of methyl resonances between 10 and 20 ppm lie in the expected range for the low-spin ($S = {}^1/_2$) ferric porphyrins.[17-20] The temperature dependence of these resonances is close to the expected Curie type though departure from such behavior is seen at higher temperatures (see Figure 4).

The two ferric porphyrin complexes would have different stereochemical structures, and they are expected to be in chemical exchange.[8,9] The curvature in the IPS plot observed at higher temperatures for the low-spin species (Figure 4) is perhaps a result of this exchange.[21] The iron(III) porphyrin complex that shows resonances in the 50–60 ppm range is clearly high spin. The definite stereochemical information on this complex is not at hand but this complex is very likely to be a six-coordinated (pyridine)iron(III) protoporphyrin IX chloride complex, in which the iron is axially coordinated to pyridine and chloride. In pyridine solution this complex will be in exchange with the low-spin iron(III) complex formed after the removal of the chloride by the pyridine. Figure 3a, showing an IPS vs. $1/T$ plot, testifies in a general way to the high-spin characteristics of the downfield resonances, but a more rigorous test of the pure high-spin Fe^{3+} species not involved in the exchange would be provided by IPS $\times T$ vs. $1/T$ plots, which would give straight lines with identical slopes.[14] Figure 3b shows such plots for the four downfield resonances and bring out that although the plots are straight lines and have nearly the same slopes for some, the slopes for all the

(5) LaMar, G. N. In *Biological Applications of Magnetic Resonance*; Shulman, R. G. Ed.; Academic: New York, 1979; p 305.
(6) Epstein, L. M.; Straub, D. K.; Maricondi, C. *Inorg. Chem.* **1967**, *6*, 1720.
(7) Moss, T. H.; Bearden, A. J.; Caughey, W. S. *J. Chem. Phys.* **1969**, *51*, 2624.
(8) Weightman, J. A.; Heyle, N. J.; Wiliams, R. J. P. *Biochim. Biophys. Acta* **1971**, *244*, 567.
(9) Hill, H. A. O.; Morallee, K. G. *J. Am. Chem. Soc.* **1972**, *94*, 731.
(10) George, P.; Beetlestone, J.; Griffith, J. S. *Rev. Mod. Phys.* **1964**, *36*, 441.
(11) Martin, R. L.; White, A. H. *Transition Met. Chem. (N.Y.)* **1968**, *4*, 113.
(12) Scheidt, W. R.; Geiger, D. K.; Haller, K. J. *J. Am. Chem. Soc.* **1982**, *104*, 495.
(13) Dugad, L. B.; Mitra, S. *Proc.—Indian Acad. Sci., Chem. Sci.* **1984**, *93*, 295.
(14) Behere, D. V.; Birdy, R.; Mitra, S. *Inorg. Chem.* **1984**, *23*, 1978.
(15) Dugad, L. B.; Marathe, V. R.; Mitra, S. *Proc.—Indian Acad. Sci., Chem. Sci.* **1985**, *120*, 189.
(16) Dugad, L. B.; Marathe, V. R.; Mitra, S. *Chem. Phys. Lett.* **1985**, *120*, 239.
(17) LaMar, G. N.; Walker, F. A. In *The Porphyrins*; Dolphin, D., Ed.; Academic: New York, 1978; Vol. 4, p 61.
(18) Kurland, R. J.; Little, R. G.; Davis, D. G.; Ho, C. *Biochemistry*, **1971**, *10*, 2237.
(19) LaMar, G. N.; Frye, J. S.; Satterlee, J. D. *Biochem. Biophys. Acta* **1976**, *428*, 78.
(20) Goff, H. M. In *Iron Porphyrins*; Lever, A. B. P., Gray, H. B., Eds.; Addison-Wesley: Reading, MA, 1983; Vol. 1, p 237.
(21) One of the reviewers has suggested that this curvature may also arise from dissociation of one or both pyridines as the temperature is increased. Since the measurements are being done with large excess of pyridine in solution, this possibility seems less likely.

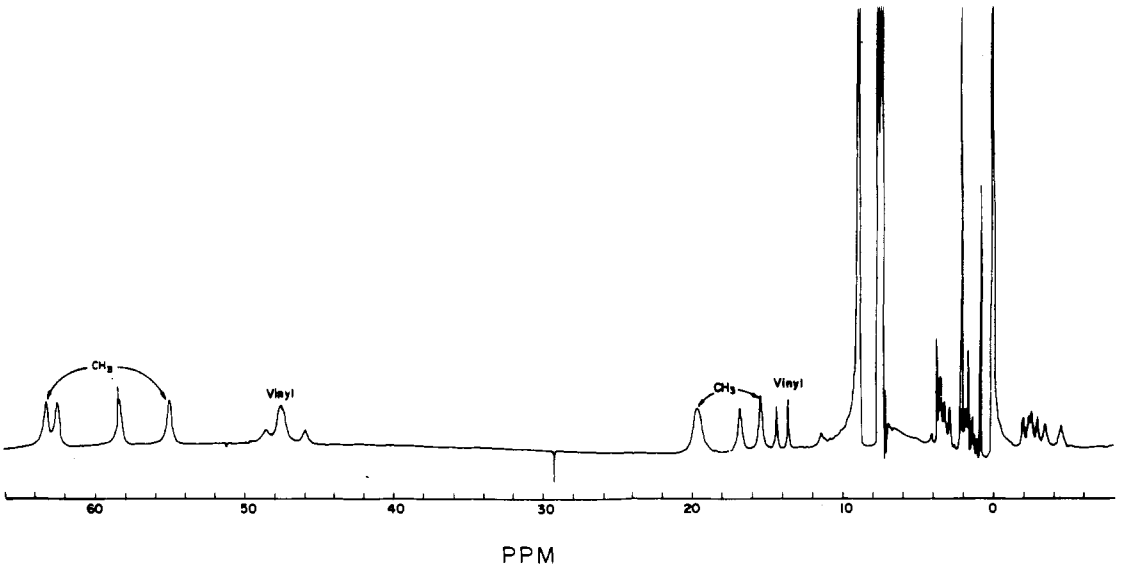

Figure 2. ^{1}H NMR spectrum of hemin chloride in pyridine-d_5 solution at 295 K. Note the methyl resonances in the 55–65 and 15–20 ppm ranges. The strong resonances in the 8–10 ppm range are due to free pyridine.

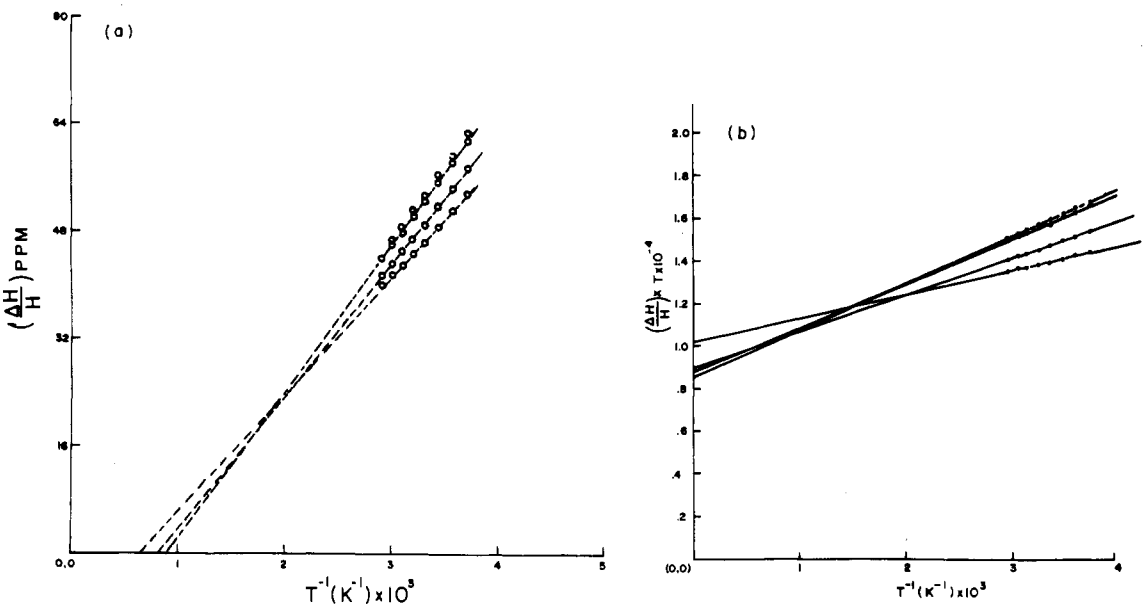

Figure 3. Temperature dependence of the downfield high-spin methyl resonances for hemin chloride in pure pyridine: (a) IPS vs. T^{-1}; (b) IPS × T vs. T^{-1}. See the text for an explanation of the latter plot.

four methyl protons are not strictly identical. Evidently this discrepancy is due to the chemical exchange that exists between the high-spin and low-spin ferric species and is expected to be slow as suggested by Weightman et al.[8] for the structural reasons. That the difference in the slopes in a sensitive plot as in Figure 3b is not very pronounced is also an evidence in favor of this exchange being slow.

It is important to digress and discuss here a very relevant aspect of the experimental result. Metalloporphyrins in general and metal protoporphyrins in particular are known for their strong tendency to aggregate in solvents of high dielectric constant and higher ionic strengths and especially in aqueous alkaline solutions.[22] At a typical concentration of ca. 50 mM, considerable aggregation is observed, leading to line broadening and shifts in the methyl and vinyl proton resonances.[23,24] However in the solvents of low dielectric constant such as dry pyridine, the tendency for aggregation is relatively weak.[25,26] We have checked the effect of aggregation by NMR of hemin chloride in pyridine solution in the concentration range 2–57 mM and did not observe any significant evidence of the porphyrin aggregation on the methyl and vinyl proton resonances.

It has been shown that the ferric ion in hemin chloride/pure pyridine solution (60 mM) is slowly reduced to bis(pyridine)-iron(II) porphyrin complex over a period of days. Our spectral results in the 20–30 mM range generally support this observation and confirm that if the measurements are made on freshly prepared solution, the amount of the reduced complex is rather small. The reduction of hemin chloride in pyridine–chloroform solution was found to be still less (Figure 5).

Hemin Chloride in Pyridine–Chloroform Solution. The ^{1}H NMR spectrum of hemin chloride in a mixture of deuteriated pyridine and chloroform solution is rather interesting (Figure 6). The sharp strong methyl resonances lying in the 15–25 ppm range

(22) White, W. I. In *The Porphyrins*; Dolphin, D., Ed.; Academic: New York, 1978; Vol. 5, p 303.
(23) LaMar, G. N.; Minch, M. J.; Frye, J. S. *J. Am. Chem. Soc.* **1981**, *103*, 5383.
(24) LaMar, G. N.; Viscio, D. B. *J. Am. Chem. Soc.* **1974**, *96*, 7354.
(25) Smith, K. M.; Bobe, F. W.; Abraham, R. J. *J. Am. Chem. Soc.* **1986**, *108*, 1114.
(26) Falk, J. E. *Porphyrins and Metalloporphyrins*; Elsevier: Amsterdam, 1964.

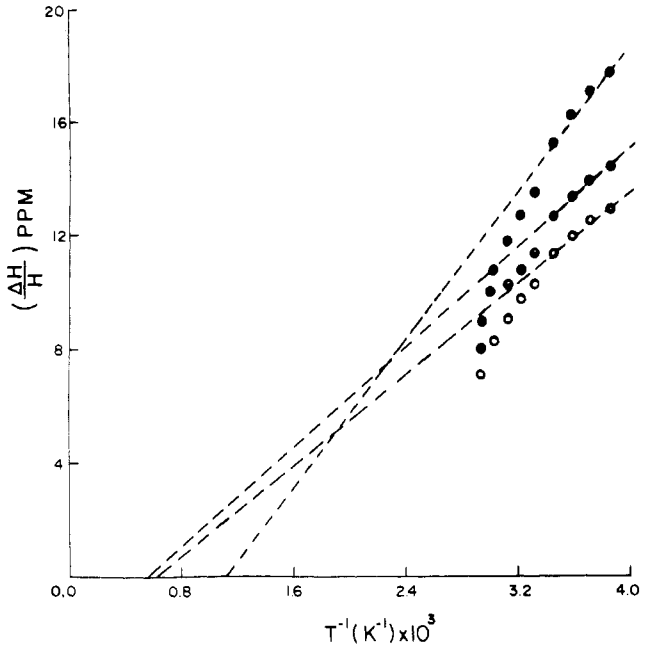

Figure 4. Temperature dependence of the low-spin methyl resonances for hemin chloride in pure pyridine.

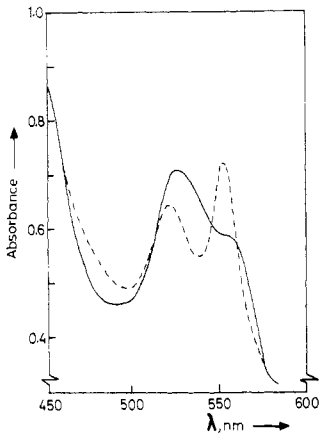

Figure 5. Visible absorption spectrum (in part) of hemin chloride in pyridine (dotted line) and pyridine–chloroform (full line) solutions.

correspond to the "low-spin" bis(pyridine)protoporphyrinato)ferric chloride and have been observed earlier by Hill and Morallee.[9] These resonances show very anomalous temperature dependence (Figure 7), which we shall discuss in detail a little later. Figure 6 also shows, however, a set of four methyl resonances lying in the 50–60 ppm range, which have a clear signature of the high-spin ferric porphyrin complex and are similar to those observed in pure pyridine solution (Figure 8). Figure 6 further shows the effect of gradual addition of the $CDCl_3$ to hemin chloride in pyridine-d_5 solution. We observe that the gradual addition of $CDCl_3$ leads to the decrease in the concentration of high-spin (pyridine)hemin chloride complex with the corresponding increase in the concentration of the "low-spin" bis(pyridine) complex. The high-spin complex is however present in this solution mixture over a large range of chloroform concentration and disappears only at a very high concentration of chloroform. Thus we conclude that hemin chloride in the mixtur of pyridine and chloroform solution stabilizes essentially the "low-spin" ferric species whose concentration increases with the increase in the amount of chloroform. Hill and Morallee[9] had mentioned, in passing, to have detected these high-spin resonances as "broad resonances from 40 to 50 ppm" but did not discuss or elaborated on it.

We further note that the autoreduction of the iron(III) hemin chloride observed in pure pyridine solution is substantially reduced in the pyridine–chloroform mixture (see Figure 5). Neither the

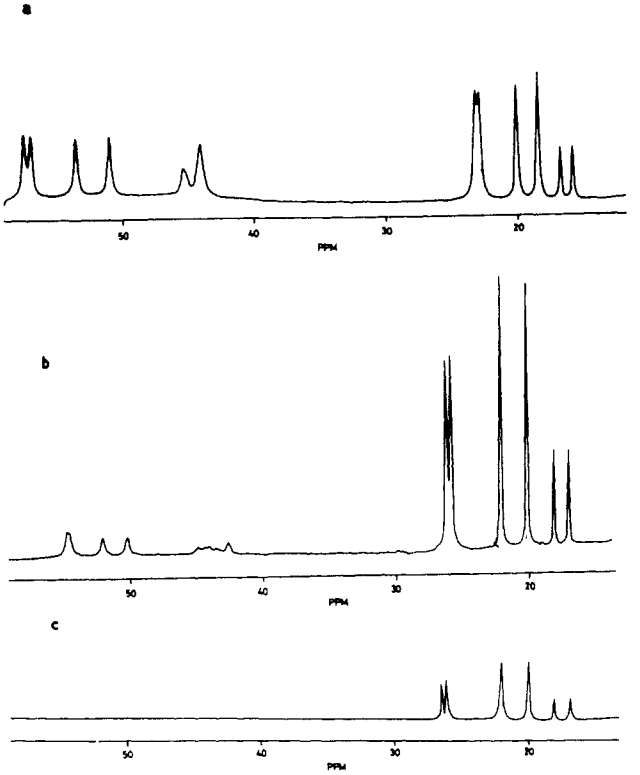

Figure 6. ^1H NMR spectrum of hemin chloride in a mixture of pyridine-d_5–chloroform with an increasing amount of chloroform. The pyridine:chloroform rations (V/V) are as follows: (a) 1:0.2; (b) 1:4; (c) 1:6.

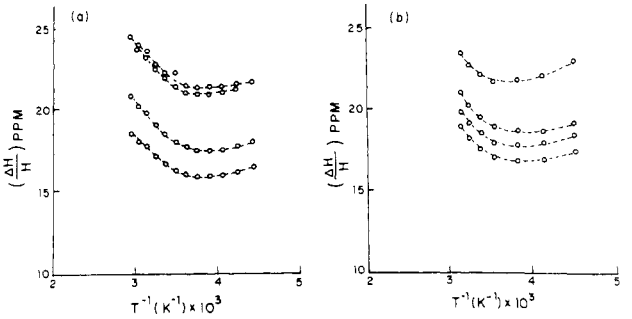

Figure 7. Temperature dependence of the "low-spin" methyl resonances of (a) hemin chloride and (b) deuterohemin chloride in pyridine–chloroform solution.

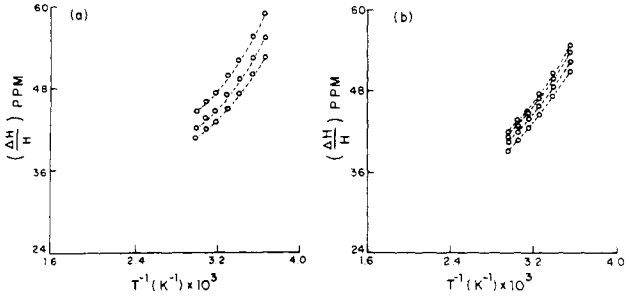

Figure 8. Temperature dependence of the high-spin methyl resonances for (a) hemin chlorode and (b) deuterohemin chloride in pyridine–chloroform solution.

optical spectral nor the ^1H NMR studies show any evidence of the formation of the iron(II) porphyrin complex in this case. Additionally, iron(III) deuteroporphyrin dimethylester chloride (which is structurally analogous to the hemin chloride) in pyridine–chloroform solution also gives evidence of the formation of only high- and "low"-spin iron(III) complexes having perhaps similar structures. Thus the carboxyl or vinyl groups do not have

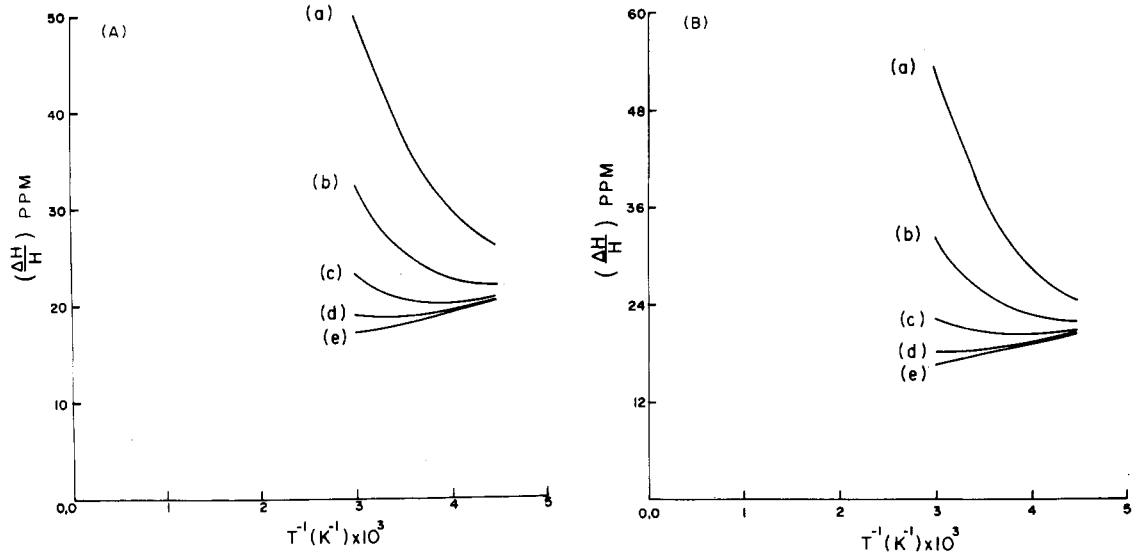

Figure 9. Temperature dependence of the calculated methyl IPS for the spin equilibrium $S = {}^5/_2 \rightleftharpoons S = {}^1/_2$ for various values of Δ (A) and vibrational partition function (B). In part A, Δ has the values (a) 800, (b) 1000, (c) 1200, (d) 1400, and (e) 1600 cm^{-1}. The vibrational partition function (ln C) and the hyperfine coupling constants (A_i) are held constant at 3.0 and 0.60 MHz, respectively. In part B the vibrational partition function has the values (a) 4, (b) 3, (c) 2, (d) 1, and (e) 0. The Δ and A_i values are held constant at 1000 cm^{-1} and 0.60 respectively.

a significant effect on the structure of the iron(III) porphyrin complexes formed here.

We now return to the "low-spin" resonances of hemin chloride in pyridine–chloroform solution. The unusual temperature dependence of the methyl IPS is very clearly marked (Figure 7) and is contrary to that expected for any ground electronic spin state of the ferric ion.[13,27] The corresponding vinyl protons also show a similar temperature dependence of the IPS. It is also interesting that almost identical temperature dependence of the IPS is shown by the metyhyl protons of Fe(DPDME)Cl in pyridine–chloroform solution. Similar behavior is also reported for the CH_2 protons in a series of $Fe^{III}(OEP)(X\text{-}py)_2ClO_4$ complexes, which has been attributed to thermal spin equilibrium between two distinct spin states of the ferric ion.[28,29] Hill and Morallee[9] had tentatively suggested that the above behavior could arise from a thermal spin equilibrium between $S = {}^3/_2$ and $S = {}^1/_2$ of the ferric ion. As mentioned in the Introduction, this equilibrium is novel and has not been observed in any heme systems as yet. It seemed therefore desirable to determine if the observed behavior could be theoretically expected for the suggested spin-equilibrium mechanism.

Theoretical calculations of the IPS were made by using an approach outlined earlier.[13-16,29] The observed isotropic shift is a combination of contact and dipolar contributions, which can be evaluated by using

$$((\Delta H)/H)_{CS} = h\sum S_i\langle S_{iz}\rangle / g_N\beta_N H$$

$$((\Delta H)/H)_{DS} = (1/3N)(K_\perp - K_\parallel)[(3\cos^2\theta - 1)/r^3]$$

Here the symbols have their usual meaning. In evaluating the contact contribution to the IPS we have allowed the hyperfine coupling constant A_i associated with each state i to be different. In determining the dipolar contribution it is quite unrealistic to calculate the principal susceptibility anisotropy ($K_\perp - K_\parallel$) by using g values, especially in situations where a number of interacting spin levels contribute in different ways to the susceptibility tensor. In the present situation we have therefore calculated[30] ($K_\perp - K_\parallel$) in terms of crystal field parameters appropriate to the models described below. The geometric factors were obtained from the known structural data. The calculation of $\sum A_i\langle S_{iz}\rangle$ is performed by an extra subroutine in the general susceptibility calculation.[30]

At first we consider the spin-equilibrium model suggested by Hill and Morallee,[9] taking $^2A_1$ and $^4A_2$ as the appropriate states corresponding to $S = {}^1/_2$ and $S = {}^3/_2$, respectively. Mixing within the two states by spin–orbit coupling and differences in the metal–ligand bonding in the two spin states were included in the theory respectively through the spin–orbit coupling parameter (ζ) and the vibrational partition function (ln C).[31,32] The calculation for this model is very similar to those reported in ref 16 except that the vibrational partition function was included in the present calculation as a further refinement. Test calculations using various sets of values of ζ, ln C, and the energy separation between $^2A_1$ and $^4A_2$ states were unsuccessful in reproducing even qualitatively the experimentally observed temperature dependence of the IPS data. The curvatures in the theoretical plots were even of opposite nature to those of Figure 7. Similarly, attempts to reproduce the experimental temperature dependence on spin-mixed model[15] between $S = {}^3/_2$ and $S = {}^5/_2$ states were also unsuccessful. The involvement of the quartet state in the iron porphyrin complexes either as the ground or the excited state has demanded a weak axial ligand like ClO_4^- of $C(CN)_3^-$.[33] Therefore the possibility of the spin equilibrium between $S = {}^1/_2$ and $^3/_2$ or of the spin-mixed $S = {}^3/_2, {}^5/_2$ states seem less likely in this case.

It is well-known that ligands like pyridine in chloroform solution give rise to the formation of pure low-spin complexes in case of synthetic hemin complexes such as Fe(TPP)Cl and Fe(OEP)Cl.[17,33] However, the bis(pyridine)(octaethylporphyrinato)iron(III) perchlorate complexes that resemble structurally with bis(pyridine)hemin chloride are not purely low-spin but show at room temperature a spin equilibrium between $S = {}^5/_2$ and $S = {}^1/_2$ states.[28,35] This seems to be a likely possibility for the system under consideration. We consider therefore a model in which thermal spin equilibrium between the $S = {}^5/_2$ and $S = {}^1/_2$ states is invoked. We assume an octahedral symmetry for the sake of simplicity and consider the equilibrium between the $^6A_1$ and $^2T_2$ states, with the latter lying lower. In this symmetry the dipolar term becomes zero. As above the effects of the vibrational partition function (ln C) and the spin–orbit coupling parameter

(27) Kurland, R. J.; McGarvey, B. R. *J. Magn. Reson.* **1970**, *2*, 286.
(28) Hill, H. A. O.; Skyte, P. D.; Buchler, J. W.; Leuken, H.; Tonn, M.; Gregson, A. K.; Pellizer, G. J. *J. Chem. Soc., Chem. Commun.* **1979**, 151.
(29) Gregson, A. K. *Inorg. Chem.* **1981**, *20*, 81.
(30) Birdy, R.; Behere, D. V.; Mitra, S. *J. Chem. Phys.* **1983**, *78*, 1453.
(31) Ewald, A. H.; Martin, R. L.; Ross, I. G.; White, A. H. *Proc. R. Soc. London, A* **1964**, *280*, 235.
(32) Golding, R. M.; Tennant, W. C.; Kanekar, C. R.; Martin, R. L.; White, A. H. *J. Chem. Phys.* **1966**, *45*, 2688.
(33) Scheidt, W. R.; Gouterman, M. In *Iron Porphyrins*; Lever, A. B. P., Gray, H. B., Eds.; Addison-Wesley: Reading, MA, 1983; Vol 1, p 89.
(34) Mitra, S. In *Iron Porphyrins*; Lever, A. B. P., Gray, H. B., Eds.; Addison-Wesley: Reading, MA, 1983; Vol. 2, p 1.
(35) Dugad, L. B.; Marathe, V. R.; Mitra, S., to be submitted for publication.

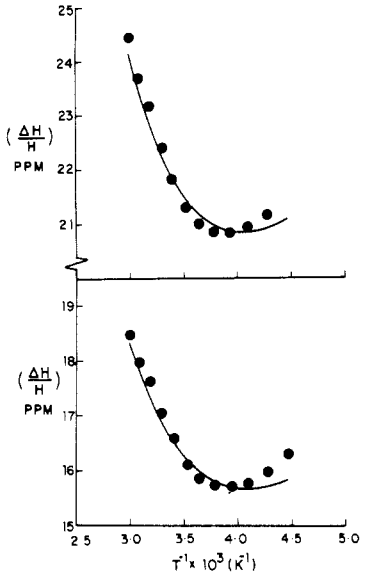

Figure 10. Temperature dependence of the experimental and theoretical IPS for two sets of "low-spin" methyl resonances of hemin chloride in pyridine–chloroform solution. The circles are the experimental data. The solid lines are the theoretically calculated ones for $\Delta = 950$ cm^{-1} and ln $C = 2$. The hyperfine coupling constants (MHz) for the upper theoretical curve are $A(^2T_{2g}) = 0.60$ and $A(^6A_1) = 0.63$, while for the lower curve $A(^2T_{2g}) = 0.45$ and $A(^6A_1) = 0.49$.

(ζ) are included. Figure 9 shows a series of test calculations with varying Δ (the energy separation between $^6A_1$ and $^2T_2$) and ln C, ζ and A_i being held constant. The results bring out the sensitive nature of these parameters to the IPS and the close similarity of the theoretical plots to the experimental data of Figure 7. From these plots, the parameter-space region of possible fits to the experimental data was delineated, which helped in obtaining the best fit to the experimentally observed temperature dependence of the methyl IPS. A result of such a fit is shown in Figure 10. The fit is good, and the values of the parameters appear reasonable. These values of parameters may not be unique since a similar fit may be obtained by a slightly different choice of Δ, ln C, and the A_i values. However, as evident from Figure 9, the range of the values of these parameters for acceptable fits to the experimental data is very narrow, and hence the present set of parameters define closely their true values. The significant point is the observation that the $S = {}^5/_2 \rightleftharpoons S = {}^1/_2$ thermal spin-equilibrium model reproduces closely the unusual temperature dependence of the IPS of the methyl protons of these complexes. It seems therefore certain that the bis(pyridine)hemin chloride complexes in pyridine–chloroform solution are not pure "low-spin" but are involved in the spin equilibrium between high- and low-spin states. The same holds true for Fe(DPDMe)Cl in the pyridine–chloroform solution as well. The present study does not however support the previous suggestion of $S = {}^3/_2 \rightleftharpoons S = {}^1/_2$ spin equilibrium.

Conclusion

The present proton magnetic resonance study shows that hemin chloride in pure pyridine contains both high- and low-spin iron(III) porphyrin complexes that are in exchange with each other. The high-spin iron(III) complex is believed to be a six-coordinated (pyridine)hemin chloride, which has one pyridine and one chloride ligand axial to the ferric ion. This is rather an uncommon stereochemistry for the iron porphyrin. The low-spin complex is the bis(pyridine)iron(III) porphyrin, in which two pyridine molecules are axially coordinated to the iron. This is a common structural form that has several analogues in the heme chemistry.[33] The addition of chloroform to this solution has a marked effect especially in very small quantities. The proton NMR spectra of Figure 6 seem to suggest a chemical equilibrium between the mono(pyridine) and the bis(pyridine) complexes since the peaks of the two complexes move toward each other as chloroform is added in small amounts.[36] The bis(pyridine)iron(III) porphyrin complex in the pyridine–chloroform solution is stereochemically the same complex as in the pure pyridine solution, but while in the pyridine–chloroform solution it shows a thermal spin equilibrium between $S = {}^5/_2$ and $S = {}^1/_2$, it behaves almost as low spin in the pure pyridine solution. Evidently the dilution of the pyridine solution with chloroform causes the subtle difference that changes the electronic structure of the bis(pyridine)ferric porphyrin complexes. Finally, it is observed that in pyridine solution the iron(III) porphyrin is slowly reduced to the iron(II) porphyrin, while in pyridine–chloroform solution this reduction is considerably less.

Acknowledgment. The NMR studies were carried out at the 500-MHz FT NMR National Facility, which is gratefully acknowledged. O.K.M. thanks Gauhati University for a leave of absence.

(36) The spectra in Figure 6 seem to provide evidence of rapid equilibrium between the high- and low-spin bis(pyridine) complexes since the peaks of the two species move toward each other as chloroform is added in small amounts. According to a reviewer, the reason for the increased rate of ligand exchange when chloroform is added could have something to do with hydrogen bonding from chloroform to the chloride ion, which could both encourage breaking the Fe–Cl bond of the mono(pyridine) complex and also help solvate the chloride ion of the bis(pyridine) complex.

Contribution from the Department of Chemistry, The University of North Carolina, Chapel Hill, North Carolina 27514

Electrocatalytic Reduction of Nitrite to Nitrous Oxide and Ammonia Based on the N-Methylated, Cationic Iron Porphyrin Complex $[Fe^{III}(H_2O)(TMPyP)]^{5+}$

Mark H. Barley, Matthew R. Rhodes, and Thomas J. Meyer*

Received July 11, 1986

An electrochemical study of the N-methylated, cationic iron porphyrin complex $[Fe^{III}(H_2O)(TMPyP)]^{5+}$ (TMPyP = *meso*-tetrakis(*N*-methyl-4-pyridyl)porphine dication) has shown that the complex is an effective electrocatalyst for the reduction of nitrite to N_2O, NH_3, and, by inference, hydroxylamine at a potential of −0.65 V (vs. SCE); reduction at −0.9 V leads to a decrease in the relative amount of N_2O produced.

Introduction

The reduction of nitrite to ammonia involves a six-electron–seven-proton change as shown in eq 1. In biological systems the

$$NO_2^- + 8H^+ + 6e^- \rightarrow NH_4^+ + 2H_2O \qquad (1)$$

$$E^\circ \text{ (vs. SCE at pH 7)} = +0.103 \text{ V}$$

net reaction is catalyzed by the nitrite reductase enzymes in which the active site is based on the iron–heme prosthetic group.[1] Although in a net sense the nitrite/ammonia interconversion is a complex reaction, relatively simple metal complexes have been

(1) Losada, M. *J. Mol. Catal.* **1975**, *1*, 245.

0020-1669/87/1326-1746$01.50/0